Revista de la Asociación Española de Materiales Compuestos
MATERIALES COMPUESTOS
http://revista.aemac.org

http://revista.aemac.org/
Vol 1, nº 1, pág. 57-64

ISSN: 2531-0739

S.M. García-Rodríguez[a], A. Bardera[b], A. Sasikumar[a],
M. Ruiz[b], V. Singery[c], I. Boada[b], D. Trias[a], J. Costa[a]

[a] AMADE, Polytechnic School, University of Girona, Campus Montilivi s/n, 17003, Girona Spain
[b] Department of Informatics, Applied mathematics and Statistics, University of Girona, Campus Montilivi s/n, 17003, Girona Spain
[c] Chomarat, 39 Avenue de Chabannes, 07160, Le Cheylard, France

Efecto del espesor de capa en la respuesta a impacto de laminados 'non-crimp-fabric' intercalados con velos: investigación por tomografía computarizada de Rayos-X

RESUMEN

Historia del artículo:
Recibido 5 de Mayo 2017
En la versión revisada 5 de Mayo 2017
Aceptado 31 de Mayo 2017
Accesible online 21 de Junio 2017

Palabras clave:
Impacto
Capas finas
Velos
Tomografía computarizada de rayos-X

Los materiales compuestos son susceptibles a cargas de impacto ya que éstas deterioran la integridad estructural de, por ejemplo, la piel del fuselaje de un avión. Por tanto, nuestro objetivo es mejorar la resistencia y tolerancia al daño de laminados finos (2.14-2.16 mm thickness) manufacturados con 'non-crimp-fabrics' (NCF) (a) reduciendo el espesor de capa convencional (considerando 'thin-plies' [1]) (b) intercalando velos no-tejidos —'non-woven veils' [2]) de fibra de co-poliamida en las intercaras de laminados con capas finas. Para ello, hemos realizado ensayos de impacto, compresión después de impacto (CAI) e indentación cuasi-estática. Además, inspecciones por tomografía computarizada de rayos-X ilustran cómo grietas en la matriz, deslaminaciones y rotura de fibra interaccionan durante impacto e indentación.

Reducir el espesor de capa disminuye el tamaño de grietas y deslaminaciones a costa de una rotura de fibras prematura, disminuyendo la tolerancia al daño. Por otra parte, intercalar velos en laminados de capas ultradelgadas evita la iniciación de deslaminaciones y aumenta la resistencia a CAI.

Effect of ply-thickness on the impact response of interleaved thin-ply non-crimp-fabric laminates: X-ray tomography investigation

ABSTRACT

Keywords:
Impact
Thin-ply
Interleaving
X-ray micro-computed tomography

Composite laminates subjected to out-of-plane loads develop damage modes that compromise the load-carrying capacity, as in the fuselage skin of an aircraft. Therefore, we aimed to improve the damage resistance and tolerance of carbon/epoxy thin non-crimp fabric (NCF) laminates by (a) reducing the 'conventional' ply-thickness (i.e. comparing thick- and thin-plies) (b) interleaving co-polyamide (CoPA) non-woven veils at the interlaminar regions of thin-ply systems. We devised an impact, compression after impact (CAI) and quasi-static indentation (QSI) experimental campaign, where computerized X-ray tomography provided detailed 3D insight on how matrix cracking, delamination and fibre failure interacted during impact and QSI.

Thin-ply laminates reduce the amount of matrix cracking and delamination at the cost of premature fibre breakage, therefore decreasing the damage tolerance. Interleaving CoPA veils arrests delamination onset and improves the residual strength with respect to the thin-ply baseline.

Autor de contacto: S.M. García-Rodríguez
e-mail: sgarciarodriguez91@gmail.com

1 Introduction

The Achilles' heel of composite laminates is their out-of-plane response, especially with the advent of time and cost-efficient resin infusion methods that decrease the quality of the finished product [3]. During service, low-velocity impacts yield to matrix cracking, delamination and fibre breakage that penalizes the integrity of laminated components [4], [5].

Some studies report that the use of 'thin-plies' (i.e. plies thinner than 150 μm [1]) improve the damage tolerance of certain material systems [6]–[8]. Under impact, they delay matrix cracking and delamination [8] at the cost of extended fibre breakage [9], [10]. However, as it usually occurs in material science, strength and toughness are mutually exclusive [11]; Frossard G. *et al.* (2016) [12] and Teixeira R.F. *et al.* (2016) [13] have demonstrated that reducing the ply-thickness decreases the inter- and intra-laminar fracture toughness.

Then, an optimal design of damage-tolerant components using thin-plies claims for the use of toughening methods [14]. In our study, we will focus on an innovative toughening approach: interleaving by 'non-woven veils' [3]. The use of this light additive may improve the compression after impact strength (CAI) [15]–[17] without concomitant reduction of other material properties [3]. In addition, they are cheap and easy to handle during manufacturing [3].

The aim of this paper is (a) compare the damage mechanisms and damage tolerance of carbon/epoxy thin laminates manufactured with thick- or thin-ply non-crimp-fabrics (NCFs) (b) understand the effect of interleaving co-polyamide (CoPA) non-woven veils in the damage tolerance of thin-ply systems. We selected laminates thinner than the standards (i.e. ~2.16 mm rather than the conventional 4 mm [18]) since the aircraft industry tends to reduce the thickness of airplane's components; for example, the skin of the Airbus A350 is less than 2 mm thick. To this end, we performed an impact, quasi-static indentation (QSI) and CAI experimental campaign. Damage induced by out-of-plane loading was inspected by X-ray micro-computed tomography (μCT) to obtain detailed insight of the damage characteristics.

2 Materials and Methods

2.1 Materials and Manufacturing

The material investigated was T700GC carbon in the form of bi-axial NCFs: 'C-ply™' from Chomarat. [0°/+45°] and [0°/-45°] fabrics of 268 and 134 g/m^2 fibre areal weight were considered (134 and 67g/m^2 per ply; thick- and thin-plies). C-plies™ were infused with the HexFlow® RTM6 epoxy resin.

A low density 'non-woven veil' of confidential properties was introduced at the interlaminar region of thin-ply laminates, namely V_2. It was made of dispersed co-polyamide fibres with melting temperature lower than the post-curing temperature (180 °C). Additionally, V_2 had 4 g/m^2 fibre areal weigth.

All the layups were manufactured by Resin Transfer Moulding (RTM). Two $[(45/0)/(-45/90)]_{ns}$ laminates were manufactured using plain carbon reinforcement: LTHICK and LTHIN (n=2 and n=4, respectively). Additionally, one $[(45/V_2/0)/V_2/(-45/V_2/90)V_2]_{4s}$ layup was manufactured by interleaving V_2 veils at every interface: LV2. The nominal laminate thickness of LTHICK, LTHIN and LV2 was 2.14-2.18 mm and their fibre volume fraction 55.9, 56.22 and 53.1%.

2.2 Experimental Methods and Damage Inspection

Impact tests were based on the ASTMD7136/D7136M–15 standard [19]. Testing was performed in a CEAS Fractovis Plus 7536 drop-weight tower with a 16 mm diameter hemi-spherical impactor. 100x150 mm (width and length) specimens were tested following the same experimental set-up than González E. *et al.* (2014) [5]. Two specimens of every batch were impacted at 10 J and one at 14 J energy.

QSI tests were performed using an electromechanical MTS INSIGHT®100 testing machine with a 10 kN load-cell. Indentation was conducted at a rate of 0.5mm/min to avoid dynamic effects. The same boundary conditions and hemi-spherical indenter were considered during impact and QSI so that both experiments yielded similar damage characteristics [20]–[22]. Three specimens per material system were tested; each of them indented to a different displacement level (d= 4, d= 4.4 and d= 5.24 mm). The higher deflection corresponds to the observation of fibre failure at the bottom-ply of LTHIN.

CAI tests were performed using an electromechanical MTS INSIGHT®300 testing machine with a 300 kN load cell. A non-standard CAI device was manufactured based on Remacha M. *et al.* (2015) [23] (a)). Because of its design, this fixture ensures local buckling-induced failure and allows damage propagation perpendicular to the applied load. CAI strengths were normalised to the volume fraction of LTHIN. Every impacted specimen was tested under compression; additionally, two pristine specimens were considered per material system.

Every indented specimen and representative impacted specimens were inspected by μCT. To improve the signal-to-noise ratio, indented specimens were cut through-the-width prior to inspection (Figure 1b)) [24]. The use of penetrant dies was avoided to ensure that matrix cracking and delamination were observed regardless their interconnection.

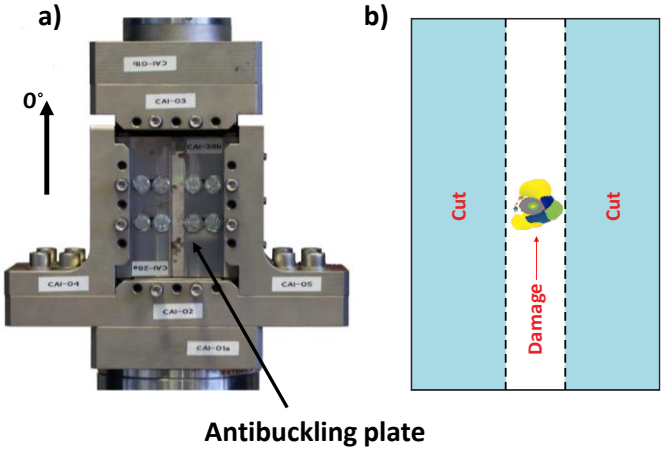

Figure 1 a) Non-conventional compression after impact (CAI) test fixture (based on Remacha M. *et al.* (2015) [23]) b) Specimens cutting prior to inspection by micro-computed tomography (μCT)

In indented specimens, the position of the inspected sample with respect to the X-ray souce and the detector was adjusted to observe the totality of the damage scenario (as previously observed by C-scan). This yielded to voxel sizes of 5 μm (d= 4 and 4.4 mm) and 7 μm (5.24 mm). In impacted specimens, only a detailed zone centred at the impact point was observed; voxel sizes of 6.5 and 10 μm for 10 and 14 J energy. Finally, in some cases, damage mechanisms were represented in 3D using the software Starviewer [25].

3 Results

3.1 Micro-Computed Tomography (μCT) results

The Figure 2 presents the μCT results of indented and representative impacted THICK specimens. In all cases, we observed resin accumulations ('resin pockets') of up to 1 mm characteristic size dispersing through-the-volume of inspection (see, for example, the Figure 2a)). In THICK indented specimens, damage localized at the bottom two-thirds of the plate (Figure 2 a), b) and c)). The exception to this was the laminate indented at d = 5.24 mm, where fibre failure developed under the impact site because of compressive stresses. In general, the damage pattern consisted on (i) 'tensile cracks' induced by tensile stresses at the bottom sub-laminates [21] (ii) 45° matrix cracks [10] (iii) matrix crack-induced delaminations (MCID, [26]). In impacted specimens, damage grew through-the-thickness of the laminate and extended several mm away from each side of the impacted point.

The Figure 3 presents the μCT results of indented and representative impacted LTHIN specimens. Halving the ply-thickness reduced the size of resin pockets by at least a factor of two (see, for example, the Figure 3a)). At d = 4 and 4.4 mm, thin-ply specimens concentrated damage at the bottom-half of the laminate and exhibited reduced MCID compared with THICK (Figures 2 and 3a)-b)). Additionally, they limited tensile cracks to the bottom-ply (the observation of this damage mechanism was blurred by their narrow crack-opening). At d= 5.24 mm, fibre breakage (iv) and fibre pull-out (v) developed at the lower third of the laminate, while matrix cracks and induced delaminations extended from the bottom to the top (see Figures 3a), b) and c)).

At 10 J, damage under the impact site of LTHIN specimens localized to a narrower region than that developed in THICK (Figures 2 and 3d)). In contrast, fibre failure extended through-the-thickness. Further increasing the impact energy caused catastrophic fibre failure which induced large delaminations compared with the thick-ply system (Figures 2 and 3d)).

The Figure 4 presents the μCT results of indented and representative impacted LV2 specimens. At d= 4.4 mm, the toughened system exhibited increased density of matrix cracks than LTHIN at the lower half of the laminate (Figures 3 and 4b)). At d=5.24 mm, matrix cracks/MCID developed through-the-thickness forming a 'cone shape' [27]. They exhibited increased crack-openings and a higher extension than these propagated in the plain material (Figures 3 and 4c)). In contrast, interleaving constrained fibre failure to the bottom-ply.

At both impact energies, LV2 reduced the severity of fibre breakage and constrained the damage to a narrow region below the impact centre relative to LTHIN (Figures 3 and 4 d)-e)). On the other hand, we observed that delamination propagation within the interleaved system decreased with increased strain rate (see μCT cross-sections of specimens indented at d= 5.24 mm and impacted at 10 or 14 J, the Figure 4c)-e)).

3.2 Compression After Impact (CAI)

The Figure 5 illustrates the CAI strength of pristine and impacted LTHICK, LTHIN and LV2 laminates. The difference between the residual strength of thick- and thin-ply specimens accentuated as the severity of fibre breakage increased in the latter system: 4.9% and 53.2% difference after 10 and 14 J impact. On the other hand, interleaving with V_2 veils enhanced the CAI strength with respect to the thin-ply baseline (16% and 22% improvement after 10 and 14 J impact, respectively)

4 Discussion

4.1 Effect of ply-thickness

NCF laminates inherently present resin accumulations since the stitching deviates the carbon tows from the uniform directions [28]. Accordingly, reducing their ply-thickness decreases the magnitude of the resin pockets as the length of the stitch between two adjacent plies also decreases. On the other hand, composites manufacturing is a scale-dependant process [9]. Microstructural defects such as fibres misalign-ments, waviness or resin accumulations augment with the size of the manufactured component (or, in this case, the ply-thickness).

Based on μCT observations in Figures 2 and 3, the damage sequence of LTHICK and LTHIN could be summarized as:

LTHICK

- Development of tensile cracks in the lower sub-laminate groups
- Growth of matrix cracks and induced delaminations from the bottom to the top parts of the laminate

LTHIN

- Development of tensile cracks at the bottom-ply
- Growth of reduced matrix cracks and delamination from the bottom to the top parts of the laminate
- Fibre failure localized at the bottom-half
- Growth of fibre failure bottom-to-top and enlargement of existing delaminations

Comparing μCT results of LTHICK and LTHIN indented specimens, we conclude that thin-ply systems delay or mitigate the development of matrix cracks and induced delaminations relative to their thicker counterparts (Figures 2 and 3a)-c)) [8], which is attributed to the increased in-situ strength [29], [30]. In contrast, the absence of delamination propagation entails lower energy dissipation and higher stress concentration in the fibres. Accordingly, fibre failure occurs when tensile stresses induced by bending overcome the fibre tensile strength at the bottom part of the laminate [6].

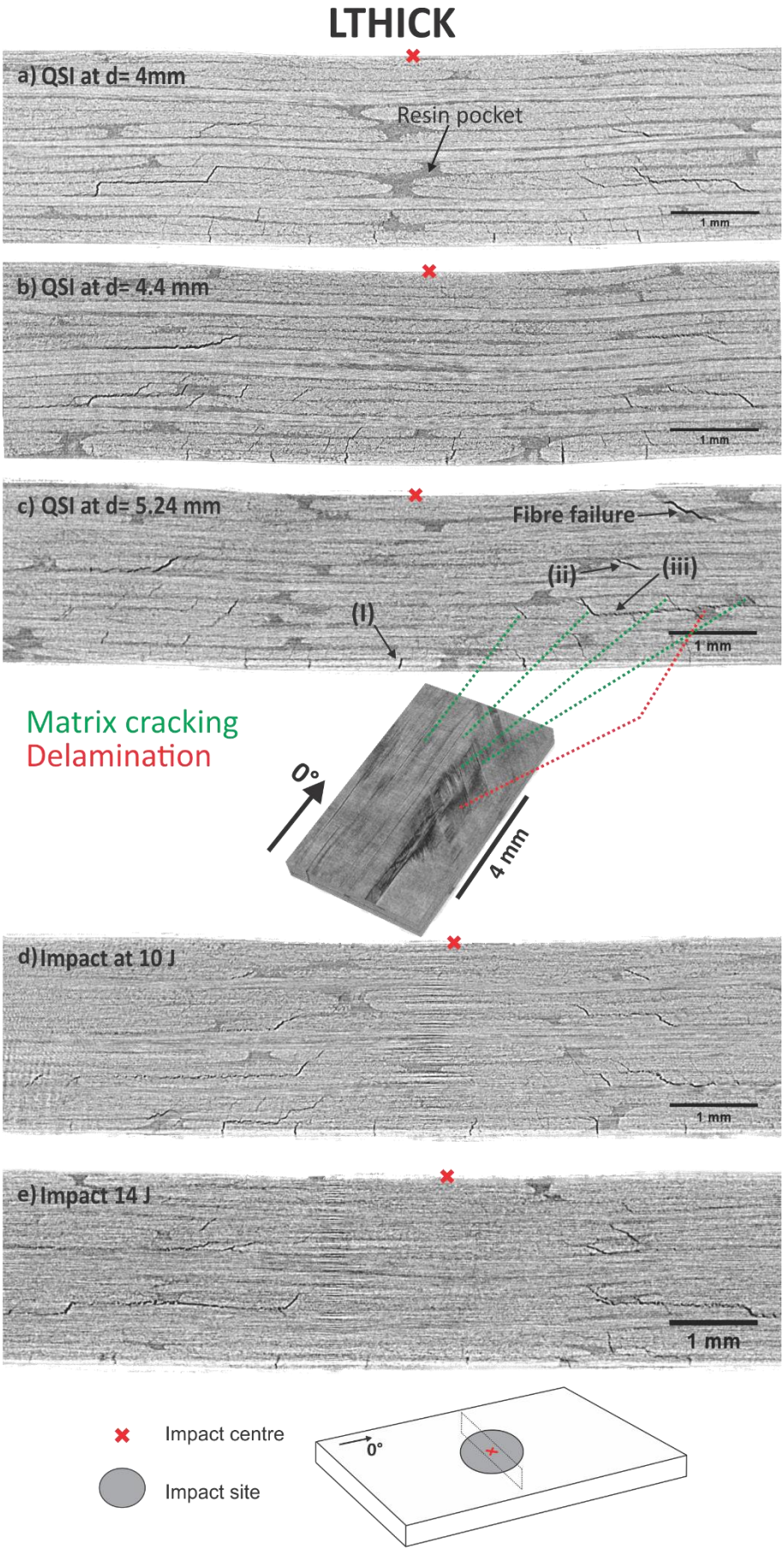

Figure 2 µCT cross-sections and 3D representative damage mechanisms of LTHICK specimens

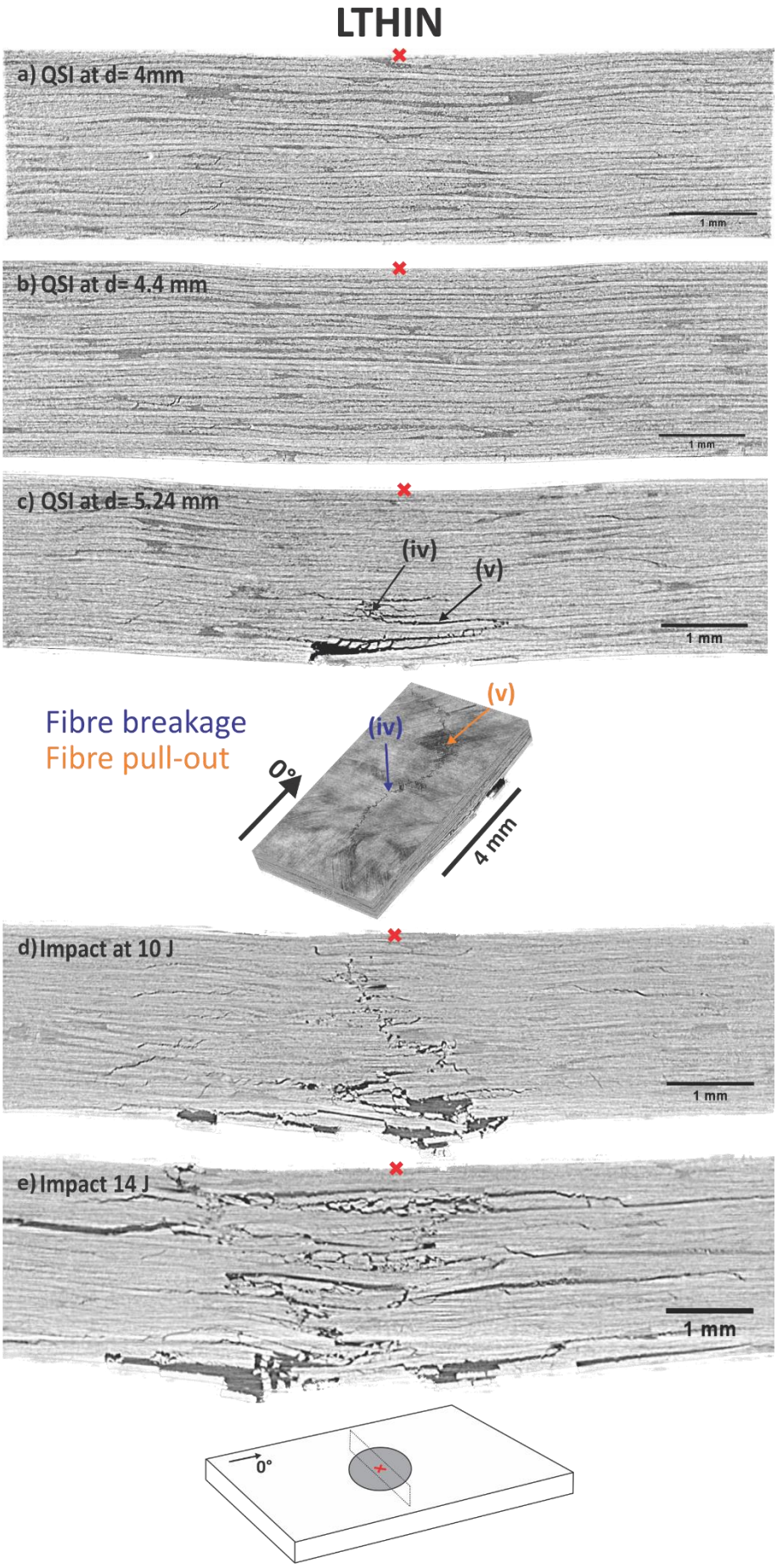

Figure 3 μCT cross-sections and 3D representative damage mechanisms of LTHIN specimens

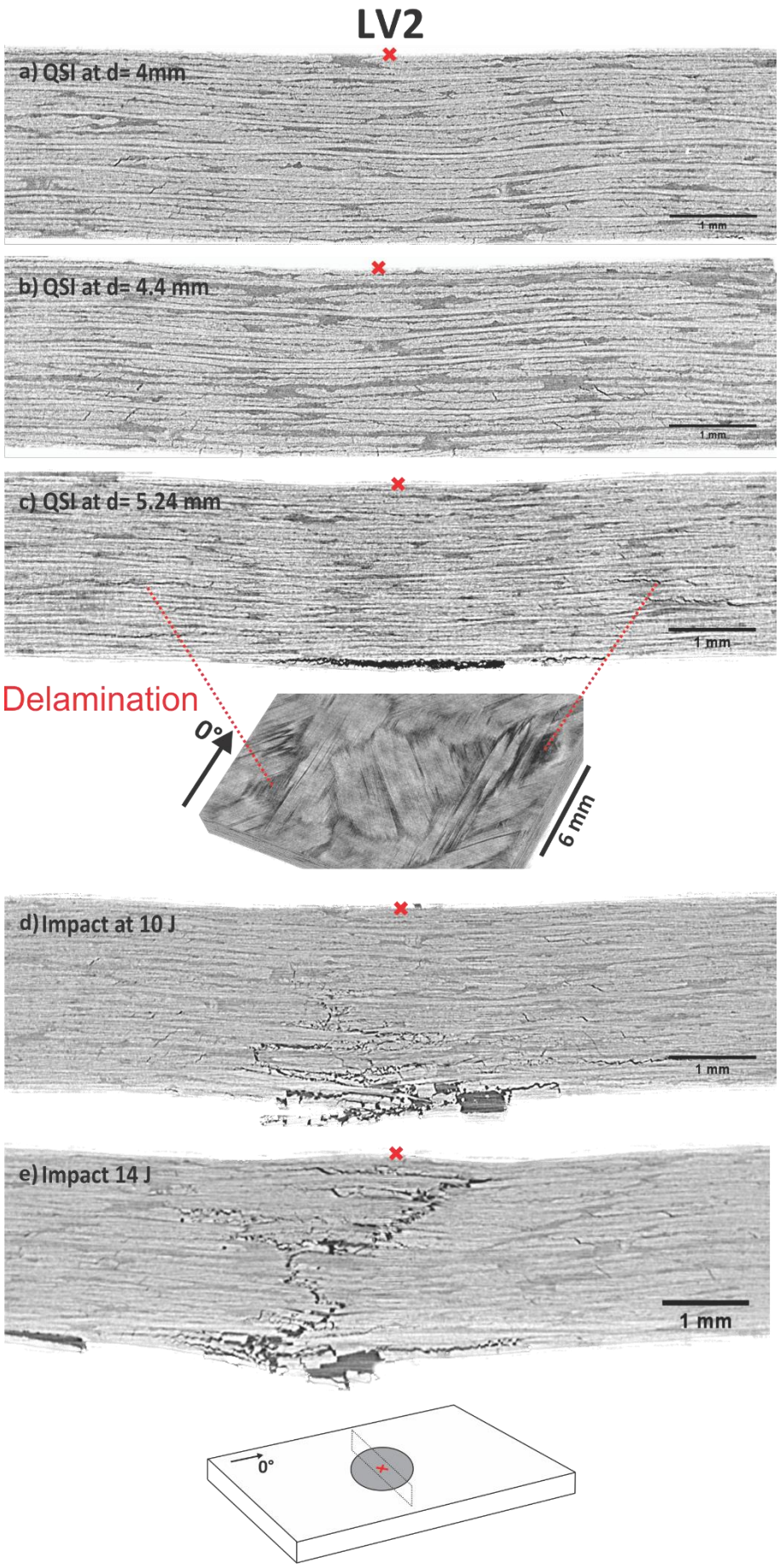

Figure 4 μCT cross-sections and 3D representative damage mechanisms of LV2 specimens

In both types of thin laminate, damage started at the bottom part of the specimen and grew upwards leading to a 'reverse pine-tree' pattern [27]. This is because the thickness of the plate is small compared to the rest of dimensions (i.e. ~2x100x150 specimens); therefore, bending and membrane effects to predominate over shear [31].

Differences between the residual strength of thick- and thin-ply materials seem to be governed by the severity of fibre breakage: the higher the amount of this damage mechanism the lower the CAI strength of LTHIN with respect to LTHICK (Figure 5). One idea could be hybridizing both types of plies in order to avoid fibre breakage while taking advantage of crack suppression.

4.2 Effect of interleaving V_2 veils

μCT slices of LTHIN and LV2 impacted specimens evidence that interleaving reduces the amount of delamination with respect to the thin-ply baseline (Figures 3 and 4d)-e)). Since the melting temperature of V_2 veils is lower than the processing temperature, they melt partially/completely at the interfaces and likely increase the interlaminar fracture toughness. This improves the damage resistance (Figures 3 and 4d)-e)) and the CAI strength (Figure 5). In fact, Nash N.H. et al. (2016) reported that non-woven veils increase the damage resistance and tolerance of carbon/Benzoxazine laminates because an improvement on the Mode II and I interlaminar fracture toughness, respectively.

Despite to the higher energy applied to the system, LV2 specimens indented at d= 5.24 mm presented more extended delaminations than layups impacted at 10 J, evidencing that thermoplastic materials are sensitive to the strain-rate [11]. Carbon/epoxy laminates toughened with thermoplastic particles also present an analogous effect when comparing QSI and impact experiments [32].

5 Conclusions

- Thin laminates manufactured with thin-ply NCFs exhibit reduced matrix cracking and delamination until fibre breakage triggers further damage extension
- Thin laminates manufactured with thin-ply NCFs decrease the damage tolerance of their thicker counterparts
- Hybridizing thick and thin-plies could be an alternative to pre-locate certain damage mechanisms and improve the 'conventional' damage tolerance
- Interleaving thermoplastic co-polyamide non-woven veils mitigate the onset of delaminations and improve the damage tolerance of thin-ply NCF systems

Acknowledgements

We greatly acknowledge the entreprise Chomarat (Le Cheylard, France) for providing the material neccesary for this study. We also acknowledge the Spanish governement through the Ministerio de Economía y Competitividad co-funded by the UE (FEDER program) under the contract MAT2015-69491-C3-1-R. The first author is particularly grateful for the support of the Secretaría de Universidades e Investigación del Departamento de Economía y Conocimiento of the Governement of Catalonia with the pre-doctoral grant 2016 FI-B00551.

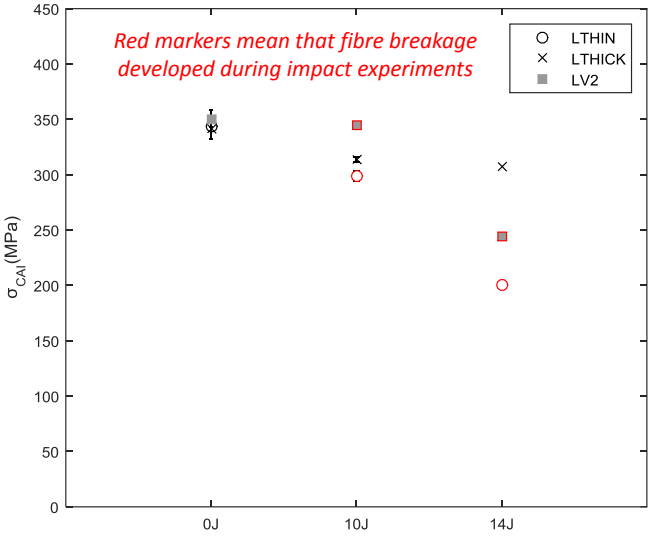

Figure 5. CAI strength of pristine and impacted LTHICK, LTHIN and LV2 specimens. The vertical bars refer to the scatter between tests

References

[1] S.Sihn, R.Y. Kim, K.Kawabe and S.W. Tsai, *Compos. Sci. Technol.*, vol. **67**, no. 6, pp. 996–1008 (2007). https://doi.org/10.1016/j.compscitech.2006.06.008

[2] V.A.Ramirez, P.J.Hogg and W.W.Sampson, *Compos. Sci. Technol.*, vol. **110**, pp. 103–110 (2015). https://doi.org/10.1016/j.compscitech.2015.01.016

[3] N.H.Nash, T.M.Young, P.T.McGrail and W.F. Stanley, *Mater. Des.*, vol. **85**, pp. 582–597 (2015). https://doi.org/10.1016/j.matdes.2015.07.001

[4] E.V.González, P.Maimí, P.P.Camanho, C.S.Lopes and N. Blanco, *Compos. Sci. Technol.*, vol. **71**, no. 6, pp. 805–817 (2011). https://doi.org/10.1016/j.matdes.2015.07.001

[5] E.V.González, P.Maimí, J.R.Sainz de Aja, P.Cruz and P.P.Camanho, *Compos. Struct.*, vol. **108**, no. 1, pp. 319–331 (2014). http://dx.doi.org/10.1016/j.compstruct.2013.09.037

[6] T.Yokozeki, A.Kuroda, A.Yoshimura, T.Ogasawara and T.Aoki, *Compos. Struct.*, vol. **93**, no. 1, pp. 49–57 (2010). doi:10.1016/j.compstruct.2010.06.016

[7] T.Yokozeki, Y.Aoki and T.Ogasawara, *Compos. Struct.*, vol. **82**, no. 3, pp. 382–389 (2008). doi:10.1016/j.compstruct.2007.01.015

[8] H.Saito *et al.*, *J. Reinf. Plast. Compos.*, vol. **30**, no. 13, pp. 1097–1106 (2011). doi: 10.1177/0731684411416532

[9] R.Amacher, J.Cugnoni, J.Botsis, L.Sorensen, W.Smith and C.Dransfeld, *Compos. Sci. Technol.*, vol. **101**, pp. 121–132 (2014). http://dx.doi.org/10.1016/j.compscitech.2014.06.027

[10] A.Wagih *et al.*, *Compos. Part A Appl. Sci. Manuf.*, vol. **87**, pp. 66-77 (2016). https://doi.org/10.1016/j.compositesa.2016.04.010

[11] M.E.Launey and R.O.Ritchie, *Adv. Mater.*, vol. **21**, no. 20, pp. 2103–2110 (2009). doi: 10.1002/adma.200803322

[12] G.Frossard, J.Cugnoni, T.Gmür and J.Botsis, *Compos. Part A Appl. Sci. Manuf.*, vol. **91**, pp. 1–8 (2016). http://dx.doi.org/10.1016/j.compositesa.2016.09.009

[13] R.F.Teixeira, S.T.Pinho and P.Robinson, *Compos. Part A Appl. Sci. Manuf.*, vol. **90**, pp. 33–44 (2016). http://dx.doi.org/10.1016/j.compositesa.2016.05.031

[14] R.Amacher, J. Cugnoni *et al.*, "Toward Aerospace Grade Thin-Ply Composites" *Proc. ECCM-17, 17th Eur. Conf. Compos. Mater.* (2016).

[15] N.H.Nash, T.M.Young and W.F. Stanley, *Compos. Struct.*, vol. **147**, pp. 25–32 (2016). http://dx.doi.org/10.1016/j.compstruct.2016.03.015

[16] L.Zhu, *Chinese J. Aeronaut.*, vol. **26**, no. 3, pp. 807–813 (2013). http://dx.doi.org/10.1016/j.cja.2013.05.006

[17] P.J.Hogg, *Mater. Sci. Eng. A*, vol. **412**, no. 1–2, pp. 97–103, (2005). doi:10.1016/j.msea.2005.08.028

[18] ASTM D7137/D7137M-12 standard (2012). DOI: 10.1520/D7137_D7137M-12

[19] ASTM D7136/D7136M–15 Standard (2015). DOI: 10.1520/D7136_D7136M-15

[20] A.Wagih, P.Maimí, N.Blanco and J.Costa, *Compos. Part A Appl. Sci. Manuf.*, vol. **82**, pp. 180–189 (2016). https://doi.org/10.1016/j.compositesa.2016.04.010

[21] S.R.H.Abisset, E.F.Daghia, X.C.Sun and M.R. Wisnom, *Compos. Struct.*, vol. **136**, pp. 712–726 (2016). http://dx.doi.org/10.1016/j.compstruct.2015.09.061

[22] D.J.Bull, S.M.Spearing and I.Sinclair, *Compos. Part A Appl. Sci. Manuf.*, vol. **74**, pp. 38–46 (2015). http://dx.doi.org/10.1016/j.compositesa.2015.03.016

[23] M.Remacha, S.Sánchez-Sáez, B.López-Romano and E.Barbero, *Compos. Struct.*, vol. **127**, pp. 99–107 (2015). http://dx.doi.org/10.1016/j.compstruct.2015.02.079

[24] D.J.Bull, L.Helfen, I.Sinclair, S.M.Spearing and T.Baumbach, *Compos. Sci. Technol.*, vol. **75**, pp. 55–61 (2013). http://dx.doi.org/10.1016/j.compscitech.2012.12.006

[25] Medical imaging software 'Starviewer'. Available at: http://starviewer.udg.edu/

[26] L.Zubillaga, A.Turon, J.Renart, J.Costa and P.Linde, *Compos. Struct.*, vol. **127**, pp. 10–17 (2015). http://dx.doi.org/10.1016/j.compstruct.2015.02.077

[27] S.Abrate, *Cambridge University Press*, (2005). www.cambridge.org/9780521473897

[28] I.Verpoest and S.V. Lomov, *Compos. Sci. Technol.*, vol. **65**, no. 15–16, pp. 2563–2574 (2005). doi:10.1016/j.compscitech.2005.05.031

[29] A.Arteiro, G.Catalanotti, A.R.Melro, P.Linde and P.P.Camanho, *Compos. Struct.*, vol. **116**, no. 1, pp. 827–840, (2014). http://dx.doi.org/10.1016/j.compstruct.2014.06.014

[30] A.Arteiro, G.Catalanotti, A.R.Melro, P.Linde and P. P.Camanho, *Compos. Part A Appl. Sci. Manuf.*, vol. **79**, pp. 127–137 (2015). http://dx.doi.org/10.1016/j.compositesa.2015.09.015

[31] L.S.Sutherland and C.G.Soares, *Int. J. Impact Eng.*, vol. **31**, no. 1, pp. 1–23 (2005). https://doi.org/10.1016/j.ijimpeng.2003.11.006

[32] D.J.Bull, A.E. Scott, S. M. Spearing, and I. Sinclair, *Compos. Part A Appl. Sci. Manuf.*, vol. **58**, pp. 47–55 (2014). http://dx.doi.org/10.1016/j.compositesa.2013.11.014